Electronic Absorption and Emission Spectra of Complexes Containing Dichromium, Dimolybdenum, and Ditungsten Quadruple Bonds

Mark C. Manning and William C. Trogler*

Contribution from the Chemistry Department, Northwestern University, Evanston, Illinois 60201.
Received December 27, 1982

Abstract: Low-temperature absorption spectra of $M_2(mhp)_4$ [M = Cr, Mo, W and mhp = deprotonated 6-methyl-2-hydroxypyridine] have been recorded in the solid state and in inert-gas matrices. Each complex displays vibronic structure on the first electronic absorption band at 22 500 (M = Cr), 20 400 (M = Mo), and 18 700 cm^{-1} (M = W). Dominant progressions in the excited-state metal-metal stretching frequency of 320 (M = Cr), 400 (M = Mo), and 320 cm^{-1} (M = W) are consistent with assignment to the metal-localized $\delta \rightarrow \delta^*$ excited state. At 15 K emission spectra were recorded for $Mo_2(mhp)_4$ and $W_2(mhp)_4$. While the vibronic nature of the emitting state was similar to that seen in absorption, there was a small (600-900 cm^{-1}) energy gap between the absorption and emission origins. The Franck-Condon factor for the emission progression was also reduced significantly from that observed in absorption. Emission from a torsionally distorted $\delta \rightarrow \delta^*$ excited state is suggested. In the D_{2d} point group of the $M_2(mhp)_4$ complexes both the $\delta \rightarrow \pi^*$ and $\pi \rightarrow \delta^*$ metal-localized excitations should be dipole allowed. A shoulder on the high-energy side of the $\delta \rightarrow \delta^*$ absorption was found in $Mo_2(mhp)_4$ and $W_2(mhp)_4$ spectra. For the tungsten derivative the reduced W-W progressional frequency of 280 cm^{-1} detected does conform to the expected antibonding character of a $\delta \rightarrow \pi^*$ process. Possible assignments for other weak spectral features are discussed. Unlike previous studies of quadruply bonded complexes, we did not observe appreciable resonance enhancement of the metal-metal stretch in Raman spectra of the $M_2(mhp)_4$ complexes. This indicates the limitations of this technique for assigning the electronic spectra of quadruply bonded complexes. Finally, a correlation between the energy and intensity of the $\delta \rightarrow \delta^*$ electronic transition is noted. Situations such as third-row metals and good donor ligands lead to increased δ orbital overlap and an intense $\delta \rightarrow \delta^*$ absorption at low energy. First-row metals, cationic complexes, and especially those that contain "hard" donor ligands yield low-intensity-high-energy transitions. These two extremes can be explained according to the amount of ionic character in the $\delta \rightarrow \delta^*$ excited state.

Although there have been numerous studies of the electronic spectra of group 6 binuclear metal complexes containing quadruple metal-metal bonds,[1-3] there has been no comparative study of a homologous series of complexes that includes all three metal types. Previous work has been hampered by the lack of stable tungsten analogues. This has been especially true for bridging carboxylate complexes $M_2(O_2CR)_4$, where the chromium and molybdenum compounds are very well known, but the preparation of $W_2(O_2CR)_4$ has only been recently achieved.[4] It is noteworthy that dinuclear complexes, which contain ligand system **1**, have been prepared for all three group 6 metals.[5,6] Many of these complexes

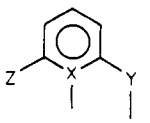

1a, Z = CH_3, X = N, Y = O
b, Z = Cl, X = N, Y = O
c, Z = H, X = N, Y = O
d, Z = OCH_3, X = C, Y = OCH_3
e, Z = H, X = N, Y = $NCCH_3$
f, Z = CH_3, X = N, Y = NH
g, Z = CH_3, X = C, Y = OCH_3

are thermally stable and sublime with minimal decomposition. These compounds also display very short (and presumably strong) metal-metal bonds.

We decided to investigate the optical spectra of complexes containing ligand **1a**, designated mhp (Hmhp = 6-methyl-2-hydroxypyridine), for a number of reasons. All three homonuclear species can be prepared, and the gas-phase He I and He II photoelectron spectra have been measured for these compounds,[7,8] as well as for the free ligand. Such data provide a reliable quantitative determination of the occupied orbital energies. The volatility of the compounds also makes them amenable to study with matrix isolation techniques and simplifies sample preparation. One can therefore examine the effect of periodicity on the low-energy $\delta \rightarrow \delta^*$ electronic transition that is characteristic of quadruple metal-metal bonds. The alternating arrangement of the bridging ligands (see Figure 1) lowers the effective symmetry to D_{2d} and eliminates the center of inversion (relative to symmetrically bridged complexes such as $Mo_2(O_2CCH_3)_4$). Transitions such as $\delta \rightarrow \pi^*$ and $\pi \rightarrow \delta^*$, which are electric dipole forbidden in D_{4h} symmetry, now should gain intensity. Recent studies of the photoreactivity of quadruply bonded systems reveal a penchant for redox chemistry from low-lying metal-localized excited states.[9] Absorption and emission spectral studies are crucial to an understanding of these phenomena.

Experimental Section

Optical spectra were recorded with a Cary 17D spectrophotometer whose sample compartment was modified to accommodate the matrix apparatus. In matrix isolation experiments, an Air Products Displex CS202B closed-cycle helium refrigerator cooled a sapphire window, affixed with indium gaskets to the cold station, to 10 K. Polycrystalline samples were set in copper grease to provide thermal contact (~15 K) with the cold station. The matrix furnace was built by the Northwestern University Physics Shop and previously described in detail.[10] Gaseous

(1) Trogler, W. C.; Gray, H. B. *Acc. Chem. Res.* **1978**, *11*, 232-239.
(2) Templeton, J. L. *Prog. Inorg. Chem.* **1980**, *26*, 211-300.
(3) Cotton, F. A.; Walton, R. A. "Multiple Bonds Between Metal Atoms"; Wiley: New York, 1982.
(4) Sattelberger, A. P.; McLaughlin, K. W.; Huffman, J. C. *J. Am. Chem. Soc.* **1981**, *103*, 2880-2882.
(5) Cotton, F. A.; Fanwick, P. E.; Niswander, R. H.; Sekutowski, J. C. *J. Am. Chem. Soc.* **1978**, *100*, 4725-4732 and references therein.
(6) Cotton, F. A.; Ilsley, W. H.; Kaim, W. *Inorg. Chem.* **1980**, *19*, 1453-1456.
(7) Garner, C. D.; Hillier, I. H.; MacDowell, A. A.; Walton, I. B.; Guest, M. F. *J. Chem. Soc., Faraday Trans. 2* **1979**, *75*, 485-493. Garner, C. D.; Hillier, I. H.; Knight, M. J.; MacDowell, A. A.; Walton, I. B.; Guest, M. F. *Ibid.* **1980**, *76*, 885-894.
(8) Bursten, B. E.; Cotton, F. A.; Cowley, A. H.; Hanson, B. E.; Lattman, M.; Stanley, G. G. *J. Am. Chem. Soc.* **1979**, *101*, 6244-6249.
(9) Nocera, D. G.; Gray, H. B. *J. Am. Chem. Soc.* **1981**, *103*, 7349-7350.
(10) Manning, M. C.; Trogler, W. C. *Inorg. Chem.* **1982**, *21*, 2797-2800.

0002-7863/83/1505-5311$01.50/0

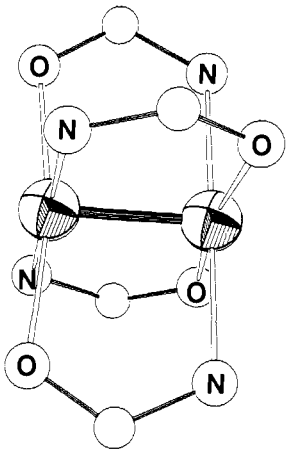

Figure 1. Molecular structure of $M_2(mhp)_4$ complexes (M = Cr, Mo, W), showing the inner coordination sphere.

Table I. Band Maxima (cm^{-1}) and Molar Extinction Coefficients for $M_2(mhp)_4$ (M = Cr, Mo, W), $Mo_2(chp)_4$,[a] Hmhp, and Hchp[a]

compd	band maxima (ϵ in M^{-1} cm^{-1})[b]
$Cr_2(mhp)_4$	α – 22 500 (480); β – 29 600 sh (~3400); γ – 33 900 (31 000); 38 000 (22 000); 43 700 (39 000)
$Mo_2(mhp)_4$	α – 20 400 (2100); β – 24 700 (12 000); γ – 35 100 (30 000)
$W_2(mhp)_4$	α – 18 700 sh (~17 000); β – 19 800 (18 500); γ – 34 500 (23 000)
Hmhp	γ – 32 300 (5700); 41 700 (7900)
$Mo_2(chp)_4$	α – 19 600 (1550); β – 24 700 (7800); γ – 35 100 (19 000)
Hchp	33 300 (160); γ – 35 700 (5200); 45 500 (6500)

[a] Hchp = 6-chloro-2-hydroxypyridine. [b] α, β, and γ bands defined in the text.

Table II. Vibronic Details for the Lowest Energy Electronic Absorption Band of Solid $Cr_2(mhp)_4$ at 15 K

origin	λ_{max}, nm	energy, cm^{-1}	ΔE,[a] cm^{-1}
A_0	474.8	21 060	0
A_1	468.0	21 370	(310)
A_2	461.0	21 690	(320)
A_3	454.3	22 010	(320)
A_4	447.8	22 330	(320)
A_5	441.7	22 640	(310)
A_6	435.5	22 960	(320)

[a] Energies in parentheses are spacings from the previous member in the progression.

argon (99.9998%), nitrogen (99.999%), and xenon (99.995%) (purchased from the Airco Corp.) were used as host matrices. Background pressure in the matrix apparatus (as monitored by a cold cathode gauge) was ca. 1×10^{-6} torr under operating conditions.

Literature methods were used to prepare $Cr_2(mhp)_4$,[5] $Mo_2(mhp)_4$,[5] $W_2(mhp)_4$,[5] and $Mo_2(chp)_4$.[6] Polycrystalline films were prepared by slow sublimation onto a sapphire window. All Raman and low-temperature (15 K) fluorescence spectra were taken of polycrystalline films. The Raman spectrometer consists of a Spex 1401 double monochromator, a Spectra Physics argon ion laser, and the requisite detection electronics. A back-scattering geometry was employed. Low-temperature emission spectra were also measured with the aforementioned apparatus, thus providing greater resolution and sensitivity than available with conventional fluorimeters.

Some low-resolution emission spectra were measured at 77 K for solid samples in 5-mm Pyrex tubes immersed in liquid nitrogen. For these experiments a Hitachi Perkin-Elmer fluorescence spectrometer was employed. Infrared spectra were obtained on a Perkin-Elmer 283 spectrometer using Nujol mull samples suspended between polyethylene plates.

Results

Absorption Spectra. Absorption spectra (Figure 2) of the $M_2(mhp)_4$ complexes (M = Cr, Mo, W) and of $Mo_2(chp)_4$ (Table I) (Hchp = 6-chloro-2-hydroxypyridine) display in each instance an absorption band system (α) below 400 nm. This lowest energy absorption red shifts and undergoes a dramatic increase in intensity (Table I) as one goes from chromium to tungsten. Each of the compounds also show an absorption (β) at higher energy (Figure 2) and the α–β separation decreases as one proceeds Cr → W. Asymmetry of the β band (Figure 1 in supplementary material) suggests that it may consist of two components. Neither band α nor β can be attributed to a purely ligand-localized transition. Band γ (Figure 2) appears in spectra of the free ligand at an

Table III. Vibronic Details for the Lowest Energy Electronic Absorption Band of Solid $Mo_2(mhp)_4$ at 15 K

origin	λ_{max}, nm	energy, cm^{-1}	ΔE,[a] cm^{-1}
A_0	507.8	19 690	0
B_0	502.0	19 920	230
C_0	500.0 sh	20 000	310
A_1	497.6	20 100	410
B_1	492.4	20 310	(390)
C_1	490.5	20 390	(390)
A_2	487.8	20 500	(400)
B_2	483.0 sh	20 700	(390)
C_2	481.0	20 790	(400)
A_3	478.5	20 900	(400)
B_3	474.0	21 100	(400)
C_3	471.8	21 200	(410)
A_4	469.7	21 290	(390)
B_4	465.2	21 500	(400)
A_5	461.2	21 680	(380)
B_5	456.2	21 920	(420)
A_6	452.6	22 090	(390)
B_6	447.5 sh	22 350	(430)

[a] Energies in parentheses are spacings from the previous member in the progression. Otherwise the spacings are relative to A_0. sh = shoulder.

Table IV. Vibronic Details for the Lowest Energy Absorption Band of Solid $Mo_2(chp)_4$ at 15 K

origin	λ_{max}, nm	energy, cm^{-1}	ΔE,[a] cm^{-1}
	537.0 sh	18 620	−690
A_0	517.9	19 310	0
A_1	508.0	19 690	300
B_1	500.7 sh	19 970	660
A_2	498.4	20 060	(370)
B_2	491.2	20 360	(390)
A_3	489.3	20 440	(390)
B_3	482.4	20 730	(370)
A_4	480.0	20 830	(390)
B_4	473.9	21 100	(370)
A_5	471.3	21 220	(390)
B_5	465.5	21 480	(380)
A_6	462.7	21 610	(390)

[a] Energies in parentheses are spacings from the previous member in the progression. Otherwise the spacings are relative to A_0. sh = shoulder.

Table V. Vibronic Details for the Lowest Energy Electronic Absorption Bands of $W_2(mhp)_4$ Isolated in a Nitrogen Matrix at 10 K

origin	λ_{max}, nm	energy, cm^{-1}	ΔE,[a] cm^{-1}
	564.5	17 710	−580
S_0	550.5	18 170	−120
A_0	546.7	18 290	0
S_1	541.5 sh	18 470	(300)
A_1	530.2	18 650	360
A_2	527.5	18 960	(310)
A_3	518.4	19 290	(330)
A_4, X_0	508.0	19 690	(400)
X_1	496.5	20 140	(270)
X_2	490.3	20 400	(300)
X_3	483.5 sh	20 680	(290)

[a] Energies in parentheses are spacings from the previous member in the progression. Otherwise the spacings are relative to A_0. sh = shoulder.

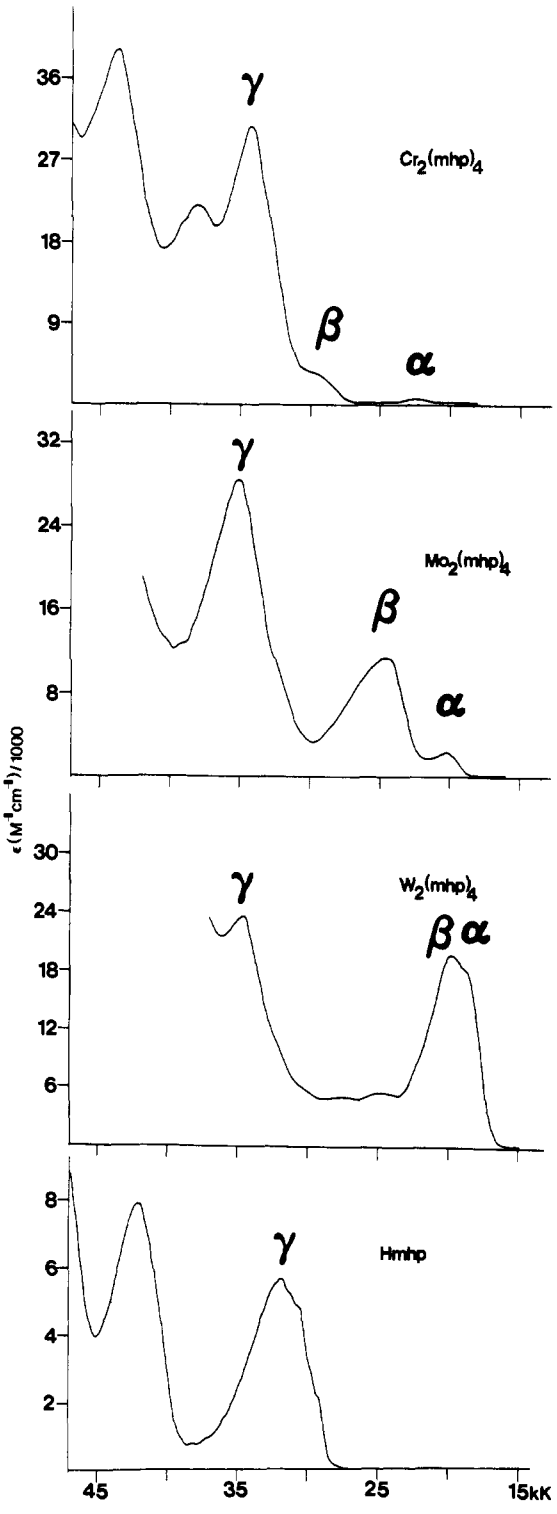

Figure 2. Absorption spectra of $M_2(mhp)_4$ (M = Cr, Mo, W) and Hmhp in tetrahydrofuran solutions.

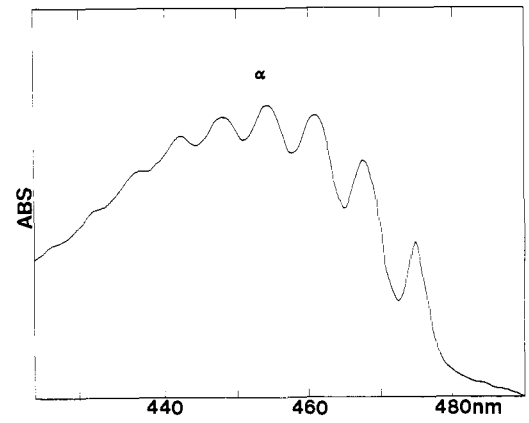

Figure 3. Electronic absorption spectrum of polycrystalline $Cr_2(mhp)_4$ on a sapphire flat at 15 K. Instrumental resolution is 0.20 nm.

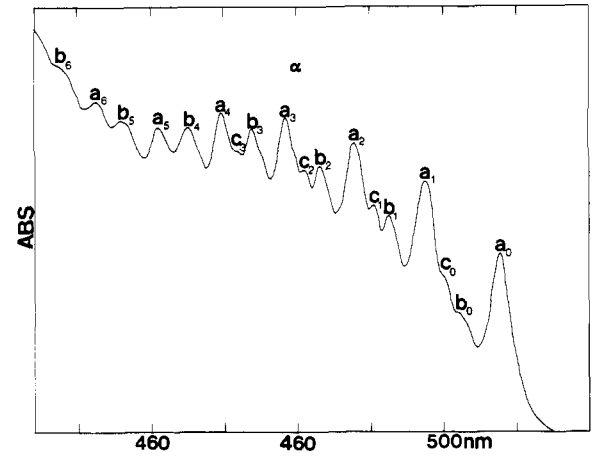

Figure 4. Electronic absorption spectrum of polycrystalline $Mo_2(mhp)_4$ on a sapphire substrate at 15 K. Instrumental resolution is 0.20 nm. The three excited-state progressions A, B, and C are designated a, b, and c, respectively.

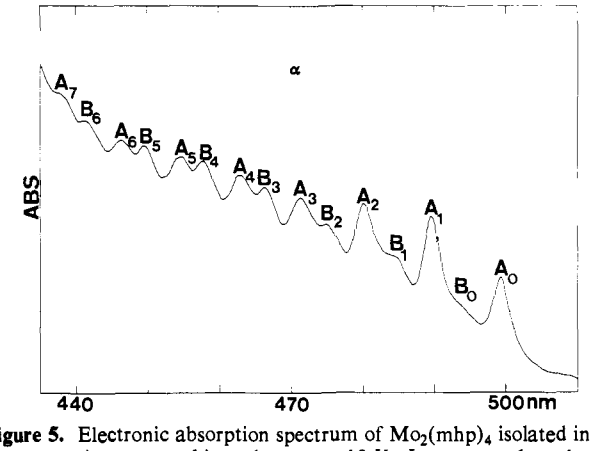

Figure 5. Electronic absorption spectrum of $Mo_2(mhp)_4$ isolated in an argon matrix on a sapphire substrate at 10 K. Instrumental resolution is 0.20 nm. Excited-state progressions are designated A and B.

intensity about one-fourth that in the complex. Assignment of this feature to a ligand-localized transition seems indicated.

At low temperature in the solid state or in rare-gas matrices, band α exhibits rich vibrational structure for $Cr_2(mhp)_4$, $Mo_2(mhp)_4$, $W_2(mhp)_4$, and $Mo_2(chp)_4$ (Figures 3–8 and figures in supplementary material). In each instance there is a long progression in a low-frequency mode (Table II–V) ~320 cm^{-1} for $Cr_2(mhp)_4$, ~400 cm^{-1} for $Mo_2(mhp)_4$, ~390 cm^{-1} for $Mo_2(chp)_4$, and ~320 cm^{-1} for $W_2(mhp)_4$.

The lowest energy absorption in complexes containing metal–metal quadruple bonds often exhibits vibrational structure with long progressions in the totally symmetric metal–metal stretching vibration.[1-3] Typically the excited-state frequencies are reduced 10–20% from the ground-state metal–metal stretching frequencies. For $Cr_2(mhp)_4$, $Mo_2(mhp)_4$, and $W_2(mhp)_4$ respective values of 556, 424, and 295 cm^{-1} have been cited for the metal–metal stretch.[4] The value of 556 cm^{-1} (touted as the highest metal–metal stretching frequency)[11] for $Cr_2(mhp)_4$ is difficult to reconcile with the excited-state data. Therefore, we examined infrared and

(11) This was the claim in ref 5, however, according to ref 3, no other chromium–chromium stretching frequency has been recorded. See Table 8.5.1 in ref 3.

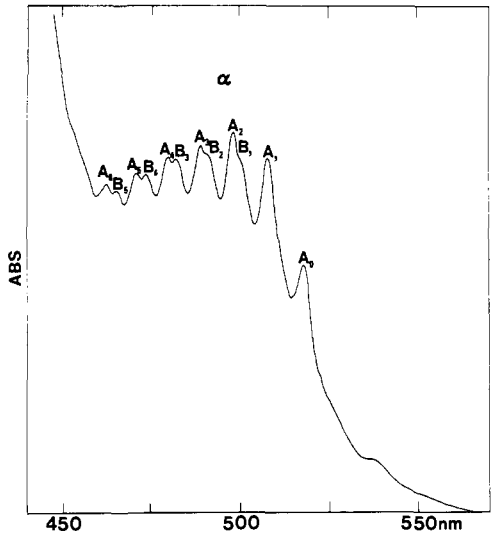

igure 6. Electronic absorption spectrum of polycrystalline $Mo_2(chp)_4$ ı a sapphire substrate at 15 K. Instrumental resolution is 0.20 nm.

able VI. Summary of Group Theoretical Selection Rules for the $_{2d}$ and D_{4h} Point Groups and a Correlation Table $D_{4h} \rightarrow D_{2d}$

D_{4h}	D_{2d}
Correlation Table	
A_{1g}	A_1
A_{2u}	B_2
A_{2g}	A_2
A_{1u}	B_1
E_g, E_u	E
$B_{1g} + B_{2g}$	$B_1 + B_2$
$B_{1u} + B_{2u}$	$A_1 + A_2$
Dipole-Allowed States (Polarization)	
A_{2u} (z)	B_2 (z)
E_u (x, y)	E (x, y)
Infrared-Allowed States:	
A_{2u}	B_2
E_u	E
Raman-Allowed States:	
A_{1g}	A_1
B_{1g}	B_1
B_{2g}	B_2
E_g	E

.aman spectra of these complexes.

By group theory (Table VI), a_1 symmetry vibrations are Raman llowed but infrared forbidden. This implies there should be an bsence of an infrared band at the metal–metal stretching freuency. In the low-frequency (<600 cm^{-1}) infrared spectrum, medium intensity band occurs at 553 cm^{-1} for $Cr_2(mhp)_4$, ıggesting that the corresponding Raman band is of e or b_2, but ot a_1 symmetry. Furthermore, a band occurs at 548–554 cm^{-1} ı the infrared and Raman spectra of all the compounds we ɛamined, including the free ligands (Table VII)! It seems quite kely that these vibrations are ligand localized. Two Raman ands, of which either may be the chromium–chromium mode,

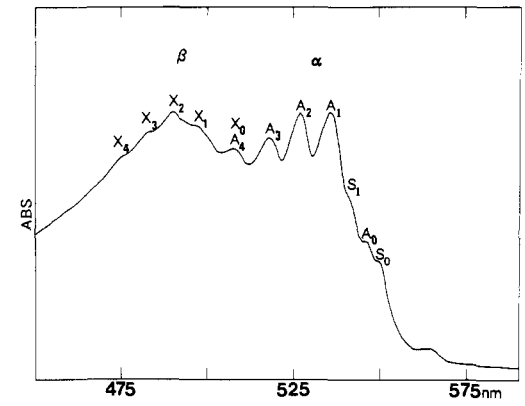

Figure 7. Electronic absorption spectrum of $W_2(mhp)_4$ isolated in a nitrogen matrix on a sapphire substrate at 10 K. Instrumental resolution is 0.20 nm.

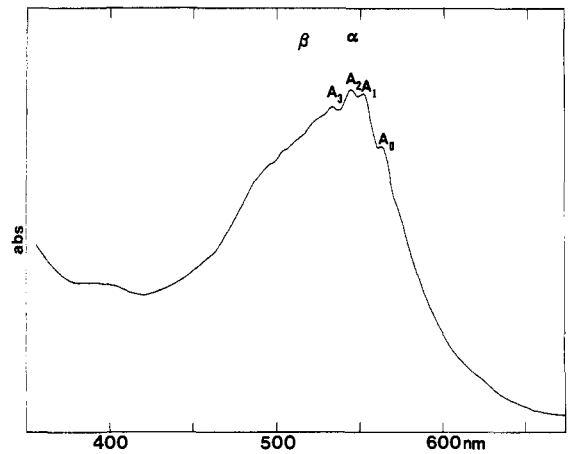

Figure 8. Electronic absorption spectrum of polycrystalline $W_2(mhp)_4$ on a sapphire substrate at 15 K. Instrumental resolution is 0.20 nm.

appear at 340 and 400 cm^{-1}. Unfortunately, we could not obtain solution spectra and determine depolarization ratios in order to further clarify the assignment.

In $Mo_2(mhp)_4$ and $Mo_2(chp)_4$ Raman lines observed at 424 and 405 cm^{-1}, respectively, do not appear in the infrared spectrum. In view of the corroborating emission spectral data (vide infra), these vibrations can be assigned to ν_{a_1}(Mo–Mo). The $W_2(mhp)_4$ complex presents a puzzle. Previous work[5] placed the ground-state tungsten–tungsten stretch at 295 cm^{-1}. Emission spectra (vide infra) seem to verify the assignement, but the progression is short and the error large. The presence of a band at 290 cm^{-1} in the infrared spectrum argues against the previous proposal; however, the relative intensity of the 290-cm^{-1} band and its similar frequency to other Re(III)–Re(III) stretches[2] does favor assignment as the tungsten–tungsten stretching vibration. The absorption spectrum reveals three excited-state progressions (Figure 7). The A spacing averages ~320 cm^{-1}, higher than the "ground-state" value of 295 cm^{-1}. Either the ground-state assignment is in error (and one of the weaker Raman bands at 325 or 360 cm^{-1} is the metal–metal stretch) or there are unusual excited-state effects.

able VII. Infrared Bands (cm^{-1}) of $M_2(mhp)_4$ (M = Cr, Mo, W), $Mo_2(chp)_4$, Hchp, and Hmhp as Nujol Mulls between Polyethylene Plates

Hchp	$Mo_2(chp)_4$	$Mo_2(mhp)_4$	$Cr_2(mhp)_4$	$W_2(mhp)_4$	Hmhp
573 m	604 s	608 s	623 sh	612 s	568 s
554 m	589 w	585 m	611 m	582 m	554 m
529 m	582 w	573 w	584 m, br	548 w	526 ms
515 m	550 w, br	548 m	553 m	406 w	510 ms
508 sh	474 w	475 w, vbr	466 mw	387 w	498 m
438 w	432 m	393 mw, br	391 s	290 ms	425 w
411 m, br	374 ms	380 w	358 vs	283 ms	325 ms, br
275 s, br	361 mw	310 s		272 m, sh	
257 sh	347 m				
	301 s, br				

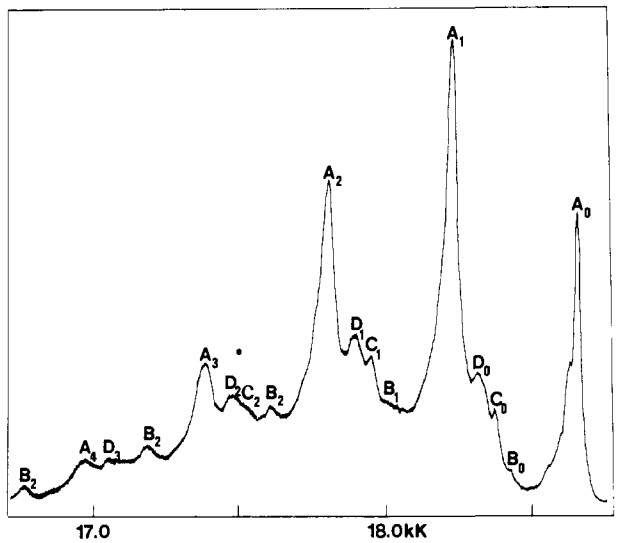

Figure 9. Emission spectrum of polycrystalline $Mo_2(mhp)_4$ on a sapphire substrate at 15 K. Instrumental resolution is 2 cm^{-1}.

Table VIII. Vibronic Details for the Emission Observed from Solid $Mo_2(mhp)_4$ at 15 K

origin	energy, cm^{-1}	ΔE,[a] cm^{-1}
A_0	18 656	0
B_0	18 429	227
C_0	18 374	282
D_0	18 317	339
A_1	18 231	425
B_1	18 012 sh	(417)
C_1	17 951	(423)
D_1	17 901	(416)
A_2	17 807	(424)
B_2	17 614	(398)
C_2	17 522 sh	(421)
D_2	17 480	(421)
A_3	17 389	(422)
B_3	17 193	(421)
D_3	17 055	(425)
A_4	16 979	(410)
B_4	16 774	(419)

[a] Energies in parentheses are spacings from the previous member in the progression. Otherwise the spacings are relative to A_0. sh = shoulder.

The merits of these possibilities will be discussed later.

One unusual aspect of the Raman studies was the absence of an appreciable resonance effect when the laser exciting line fell within the region of absorption due to band α. Dramatic intensity increases of the Raman active metal–metal stretching vibration are observed upon resonance excitation of the $\delta \rightarrow \delta^*$ absorption in $Re_2X_8^{2-}$ (X = F, Cl, Br, I) and $Mo_2X_8^{4-}$ (X = Cl, Br) compounds.[12]

While the vibronic nature of the lowest energy absorption appears similar in all four complexes studied, there are subtle distinctions. $Cr_2(mhp)_4$ exhibits a single broad progression (Figure 3) in ν_{a_1}(Cr–Cr), while the $Mo_2(mhp)_4$ complex shows three vibronic origins (a–c of Figure 4). Origins a, b, and c persist in the Ar and N_2 matrix spectra (Figure 5 and Figure 2 in supplementary material) and appear to be genuine. In the chp derivative, there are again three origins (A, B, X of Figure 6). The component X appears to belong to an electronic state distinct from that responsible for the A and B progressions. The spectrum of the tungsten complex is even more complex due to overlap of the α and β bands (Figure 7). On the α band there is a fairly regular sharp A progression of 329 cm^{-1} while the β band displays a broad X progression of 280 cm^{-1}. Furthermore, part of a second pro-

(12) Clark, R. J. H.; Franks, M. L. *J. Chem. Soc., Chem. Commun.* **1974**, 316–317. Clark, R. J. H.; Franks, M. L. *J. Am. Chem. Soc.* **1978**, *100*, 3088–3091. Clark, R. J. H.; Franks, M. L. *Ibid.* **1976**, *98*, 2763–2767.

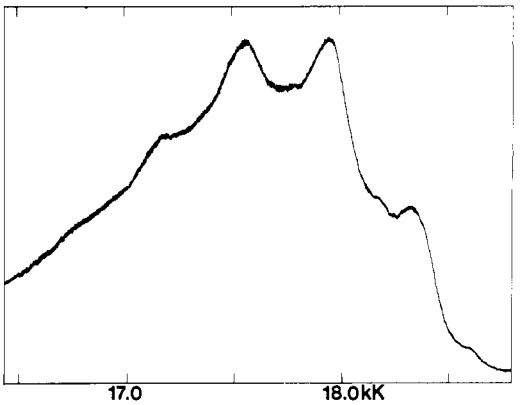

Figure 10. Emission spectrum of polycrystalline $Mo_2(chp)_4$ on a sapphire substrate at 15 K. Instrumental resolution is 2 cm^{-1}.

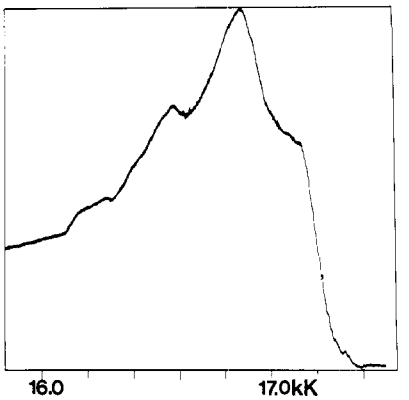

Figure 11. Emission spectrum of polycrystalline $W_2(mhp)_4$ on a sapphire substrate at 15 K. Instrumental resolution is 2 cm^{-1}.

Table IX. Vibronic Details for the Emission Observed from Solid $Mo_2(chp)_4$ at 15 K

origin	energy, cm^{-1}	ΔE,[a] cm^{-1}
E_0	18 590	−265
A_0	18 325 sh	0
E_1	18 170	(420)
A_1	17 945	(380)
A_2	17 560	(385)
A_3	17 170	(390)

[a] Energies in parentheses are spacings from the previous member in the progression. Otherwise they are relative to A_0.

Table X. Vibronic Details for the Lowest-Energy Absorption Bands of Solid $W_2(mhp)_4$ at 15 K

origin	λ_{max}, nm	energy, cm^{-1}	ΔE,[a] cm^{-1}
A_0	564.5	17 750	0
A_1	553.0	18 080	(330)
A_2	544.5	18 370	(290)
A_3	534.1	18 720	(350)

[a] Energies in parentheses are spacings from the previous member in the progression.

Table XI. Vibronic Details for the Emission Observed from Solid $W_2(mhp)_4$ at 15 K

origin	energy, cm^{-1}	ΔE,[a] cm^{-1}
A_0	17 120 sh	0
A_1	16 870	(250)
A_2	16 570	(300)
A_3	16 270	(300)
	16 180 sh	

[a] Energies in parentheses are spacings from the previous member in the progression. sh = shoulder.

Table XII. Lowest Allowed Transitions in $M_2(mhp)_4$ Complexes Descending the Table in Approximate Order of Energy (Lowest to Highest)

transition	symmetry (D_{2d} Point Group)
$\delta \rightarrow \delta^*$	$^1A_1 \rightarrow {}^1B_2$
$\delta \rightarrow \pi^*$	$^1A_1 \rightarrow {}^1E$
$\delta \rightarrow \pi^*_{lig}$	$^1A_1 \rightarrow {}^1E$
$\pi \rightarrow \delta^*$	$^1A_1 \rightarrow {}^1E$
$\sigma \rightarrow \delta^*$	$^1A_1 \rightarrow {}^1A_1$
$\pi_{lig} \rightarrow \delta^*$	$^1A_1 \rightarrow {}^1E$

gression S_0, S_1 appears on the α band. In the solid state (Figure 8), the α and β bands are not well separated, and both have red-shifted significantly. A complex band shape is observed with a barely resolved A progression.

Emission Spectra. Intense structured emission was detected from the molybdenum complexes at 15 K (Figures 9 and 10) and the progressional frequencies (Table VIII and IX) of 420 cm^{-1} for $Mo_2(mhp)_4$ and 400 cm^{-1} for $Mo_2(chp)_4$ closely correspond to ν_{a_1}(Mo–Mo) vibrations found at 424 and 405 cm^{-1} respectively in the Raman spectra. The $W_2(mhp)_4$ complex exhibited weak luminescence of somewhat poorer resolution (Figure 11); however, a ν_{a_1}(W–W) progression of roughly 290 cm^{-1} (Tables X and XI) can be discerned.

There are two important features of the emission spectra: (1) the origin of luminescence does not overlap the origin of the absorption band; (2) the shape of the emission band does not mirror the shape of the absorption band. The progression in the metal–metal stretch observed in emission dies out much sooner (by the fourth overtone) than in absorption (by the seventh to eighth overtone). Consequently, the Franck–Condon distortion in the emitting state must be much smaller than that in the absorbing state. The energy gap between absorbing and emitting states is 1030 cm^{-1} in $Mo_2(mhp)_4$, 975 cm^{-1} to $Mo_2(chp)_4$, and 600 cm^{-1} in $W_2(mhp)_4$. To ensure the authenticity of the energy gap, we checked the calibration of our absorption spectrometer with a mercury resonance lamp and found an uncertainty of ±50 cm^{-1} (at most) in the region of absorption. Emission spectral calibration (relative to lines from the argon ion laser) was much more accurate. Therefore, the energy gaps are significant.

Discussion

Two independent studies[7-9] of the gas-phase photoelectron spectra of $M_2(mhp)_4$ show that the metal-localized δ orbital is the highest occupied level and the ionization potential of the δ orbital shifts uniformly in the series chromium > molybdenum > tungsten. The greater ease of ionization reflects increased diffuseness of the δ orbitals and, consequently, improved overlap. This suggests that the δ component of the bond becomes stronger as the table is descended, despite the larger metal–metal separation. On the other hand, the IP of the σ and π levels is relatively constant in this series.

For all complexes, there is a significant δ–σ,π energy gap (1.4 eV in Cr_2; 2.3 eV in Mo_2; 2.7 eV in W_2); however, ionizations due to ligand localized π electrons overlap with the σ,π metal ionizations. As a result, the low-lying electronic transitions probably all originate from the δ-bonding level. The UV absorption spectrum could be difficult to interpret due to the close proximity of several filled orbitals, including σ,π, and at least one ligand localized π level.

Presently, there are no theoretical descriptions available for the unoccupied orbitals in $M_2(mhp)_4$ compounds or analogous bridged systems. Although this is a hindrance in determining the nature of the lowest energy excited states, some reasonable estimates can be made. As with other quadruply bonded species, the δ^* orbital is probably the LUMO. Next lowest are probably the metal-localized π^* level and π^* orbitals from the mhp ligand. As a consequence, we can roughly estimate the order of electronic transitions (Table XII) according to this scheme.

Assignment of Lowest Energy Electronic Transitions. The lowest energy absorption feature α, which bears distinct progressions in the metal–metal stretching vibration, may be assigned to the $\delta \rightarrow \delta^*$ ($^1A_1 \rightarrow {}^1B_2$) transition; this is consistent with the framework emerging[3] for other quadruply bonded binuclear complexes. Only one progressional origin is observed for $Cr_2(mhp)_4$, having a spacing of ~320 cm^{-1} (see Figure 2). This fact, in conjunction with the IR and Raman information, rules out the previous[5] 556 cm^{-1} assignment for the ground-state chromium–chromium stretch. Given the usual 10–50 cm^{-1} decrease of the metal–metal stretch in the excited state,[3] the 340 cm^{-1} Raman band appears to be the most reasonable candidate for the ground-state stretch. It is interesting to note that $Cr_2(mhp)_4$ is the first Cr–Cr system to exhibit vibronic structure on the $\delta \rightarrow \delta^*$ transition. In $Cr_2(O_2CCH_3)_4 \cdot 2H_2O$ the $\delta \rightarrow \delta^*$ absorption was not found to be the lowest energy feature in the electronic absorption spectrum.[13] The new value of 340 cm^{-1} for the Cr–Cr stretch suggests that the Cr–Cr stretching force constant is considerably less than previously estimated[3] and well below those for the analogous molybdenum and tungsten derivatives.

The molybdenum species $Mo_2(mhp)_4$ shows better resolved vibronic structure. Three distinct origins for progressions in ν_{a_1}(Mo–Mo) can be seen in the nitrogen matrix and polycrystalline samples (Figure 3 and 4), whereas in argon and xenon matrices, only two origins are apparent (figures in supplementary material). In contrast to the $Mo_2(O_2CR)_4$ series,[10] the Mo–Mo progressional frequency is nearly identical in both solid and matrix-isolated $Mo_2(mhp)_4$ compounds. The variation in ν_{a_1}(Mo–Mo) in the carboxylate case was attributed to axial interactions. Such interactions are severely hindered in the mhp derivatives due to the blocking of the axial positions by methyl subsitutents.[5] There is a small shift in the position of the zero phonon line (~300 cm^{-1}) of $Mo_2(mhp)_4$ upon changing the host lattice. Again, this is less than observed with $Mo_2(O_2CCH_3)_4$. Both B and C appear to be vibronic origins built upon the 0–0 line a_0. The spacings (a_x–b_x, ~210 cm^{-1}; a_x–c_x, ~280 cm^{-1}) are consistent with the enabling modes being metal–ligand stretches (either metal–oxygen or metal–nitrogen).

The chloro derivative $Mo_2(chp)_4$ exhibits similar spectral features. There is a slight decrease in the progressional frequency relative to $Mo_2(mhp)_4$ (by ~10–15 cm^{-1}) and only two progressional origins are observed in the thin film spectrum (Figure 6). Origin B_0 is washed out, but the odd band shape of A_1 indicates there is probably a second component present. One unusual characteristic is the presence of a weak peak in all the samples, about ~700 cm^{-1} below A_0. The relative intensity and energy spacing argue against a hot band assignment. On the basis of previous work with $Mo_2(O_2CR)_4$ species,[10] which also show anomalous weak features below the 0–0 band, we propose the weak origin is due to a spin- or dipole-forbidden electronic transition. The exact assignment will be discussed in concert with the emission spectral data.

The ditungsten species $W_2(mhp)_4$ presents a more complex situation. In this compound, the gap between $\delta \rightarrow \delta^*$ and the next states accessible by dipole transitions has collapsed to a few hundred wavenumbers. As a result, there is significant overlap between several electronic excitations. The absorption spectrum was recorded for $W_2(mhp)_4$ in solid argon and nitrogen matrices, as well as for the polycrystalline film (Figures 7 and 8 and supplementary material). Crystalline film spectra were consistently of poor quality, owing to inherent spectral broadness. It appears that band overlap is more severe in the film case than in matrix-isolated complexes. Consequently, we will focus attention on the matrix spectra.

The most distinct progression is labeled A, displaying five members, with a spacing averaging ~320 cm^{-1}. For all spectra the A_3–A_4 gap appears much larger (~400 cm^{-1}). In addition, there are pronounced shoulders (most obvious in the nitrogen spectrum) to slightly lower energy. These are labeled S_0 and S_1 (spacing ~285 cm^{-1}). Two explanations for these peaks are possible. Either A_0 and S_0 represent nonequivalent sites in the host lattice or they are separate progressions, and S_0 is the true

(13) Rice, S. F.; Wilson, R. G.; Solomon, E. I. *Inorg. Chem.* **1980**, *19*, 3425–3431.

0–0 band for the $\delta \rightarrow \delta^*$ excited state. The former alternative seems more reasonable, considering the markedly different intensities of S in several matrices. There is also a third progression which appears to originate in the vicinity of A_4 and is labeled X. Because the energy spacing is less than for A (280 vs. 320 cm^{-1}), it is assigned to vibronic structure for $\delta \rightarrow \pi^*$. A reduced progressional frequency for $\delta \rightarrow \pi^*$ compared to $\delta \rightarrow \delta^*$ seems reasonable considering the expected metal–metal antibonding character.

There remains a problem with the A progressional frequency which is $\sim$30 cm^{-1} larger than ν_{a_1}(W–W) in the ground state. As discussed previously, it is possible that the ground state assignment errs. An alternative proposal is that upon excitation, the molecule undergoes a distortion (Duschinsky effect) causing a differing mix of totally symmetric vibrations in the excited state.[14] Since the a_1 metal–ligand modes are probably higher in energy than a_1(W–W), then mixing more of their character into a_1(W–W) would increase the frequency of the "W–W stretch". As in the $Mo_2(chp)_4$ spectra, there is a weak vibronic feature in the spectrum of $W_2(mhp)_4$ at low energy. Its position is $\sim$600 cm^{-1} below the origin, so it is not a hot band. Again, we suggest it belongs to a distinct electronic state.

Emission Spectra and Assignment of Weak Low-Energy Absorption Features. In this section, we will discuss the possible explanations for the weak, absorption features observed *below* the electronic origin of $\delta \rightarrow \delta^*$, the lowest energy, dipole- and spin-allowed electronic state. Also, the nature of the emitting state will be considered. Since the chromium compound displays none of these special features, only the molybdenum and tungsten complexes are discussed.

At low temperatures, $Mo_2(mhp)_4$ exhibits a highly structured emission spectrum with four distinct origins for progressions (Figure 9). The highest energy emission line, labeled A_0, occurs at 18 660 cm^{-1}. This is 1030 cm^{-1} lower in energy than the 0–0 band of the $\delta \rightarrow \delta^*$ ($^1A_1 \rightarrow {}^1B_2$) transition (origin 19 690 cm^{-1}). Lack of overlap indicates that the emission cannot be simple fluorescence from the $^1B_2$ state. Three possible explanations must be considered. First, the luminescence may be fluorescence from the $^1B_2$ level, if that state has a severely distorted geometry in the excited state. Such an assignment has been proposed for the emission from $Mo_2Cl_8^{4-}$ and $Re_2Cl_8^{2-}$.[15,16] Second, the luminescence may be phosphorescence from the triplet portion of $\delta \rightarrow \delta^*$. Third, we are observing emission from some other spin-forbidden state.

At first glance, the emission vibrational fine structure appears to be quite similar to that of the absorption spectra. The A, B, and C progressions in emission are of similar nature of those seen in absorption for $Mo_2(mhp)_4$ and $Mo_2(chp)_4$. The major differences are that relative to A the B and C features are weaker in emission than in absorption, and the B progression behaves oddly. Its intensity seems to drop and then recoup. In addition, there is a D progression, placed $\sim$340 cm^{-1} below A. The other important difference between the absorption and emission bands is the relative Franck–Condon factors. Whereas eight or nine members of the A progression can be detected in absorption, only five are observed in emission. The metal–metal bond therefore appears to be weakened more in the ($\delta \rightarrow \delta^*$) $^1B_2$ state than in the emissive state. This could suggest that the structured absorption and emission arise from separate electronic levels.

A difference in Franck–Condon factors, or lack of "mirror symmetry", was also evident in the $M_2X_8^{n-}$ (M = Mo_2, X = Cl, n = 4; M = Re, X = Cl, Br, n = 2)[15-17] complexes and helped to rule out simple fluorescence. First, the band was assigned as the $\delta \rightarrow \delta^*$ triplet ($^1A_{1g} \rightarrow {}^3A_{2u}$).[16] This was later reconsidered because it gave a singlet–triplet splitting much smaller than anticipated by theory. Subsequent work on $Mo_2Cl_4(PBu_3)_4$ showed this compound possessed emission which was a mirror image of the absorption spectrum.[16] It was then proposed that the singlet $\delta\delta^*$ state was distorted by torsion around the metal–metal axis toward a staggered geometry. Fluorescence then need not be the mirror image of the absorption band.[14] Presumably the phosphine derivative, due to steric constraints, cannot undergo this torisonal motion and displays simple fluorescence, including overlap of the 0–0 bands.

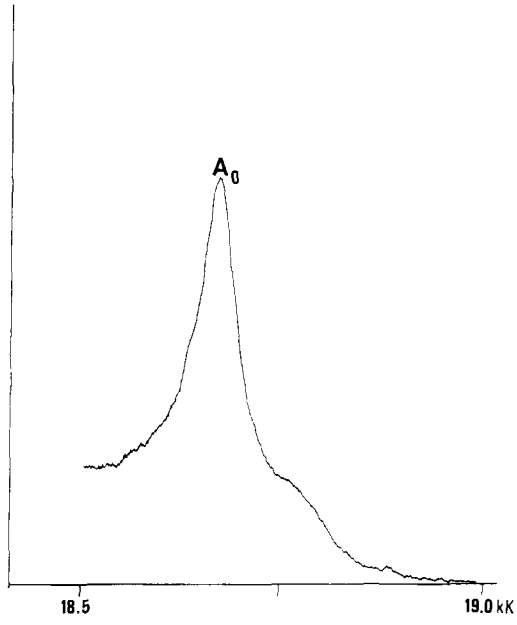

Figure 12. Expanded view of the origin of the emission from solid $Mo_2(mhp)_4$ at 15 K. Excitation was with the 4880-Å line of an argon ion laser. The shoulder is about 90 cm^{-1} below A_0. Resolution is 2.5 cm^{-1}.

Due to energy considerations, which predict the multiplet splitting of the [$\delta\delta^*$] state to be greater than 0.5 eV,[18] we dismiss the $^3[\delta\delta^*]$ ($^3B_2$) assignment for the intense luminescence. Chelation by the mhp ligands should restrict rotation about the metal–metal bond (as proposed for the halide complexes), but such a process might still occur. Although the energy gap is substantial and rotation should be restricted, the assignment of the emission to fluorescence from a twisted excited singlet state is plausible.

Another possible explanation is that emission occurs from another triplet state. According to calculations on $Mo_2(O_2CH)_4$, only the $^3[\delta\pi^*]$ (^3E) level is energetically feasible.[18] There is a drawback to this assignment as well. The Franck–Condon factor should be greater for $\delta \rightarrow \pi^*$ than for $\delta \rightarrow \delta^*$, since the former excitation disrupts metal–metal bonding to a greater extent. However, the observed emission has a reduced Franck–Condon factor. Although a triplet state should appear weakly in absorption as well as in emission, no absorption bands could be discerned in $Mo_2(mhp)_4$, even with thick films. The $Mo_2(chp)_4$ complex displays a weak absorption below A_0; however, it does not overlap with the strong emission bands. The gap between the absorption and emission electronic origins for $Mo_2(chp)_4$ is 975 cm^{-1}, slightly less than for $Mo_2(mhp)_4$. Only a single strong emission progression is seen, with a frequency averaging $\sim$400 cm^{-1}. Unlike $Mo_2(mhp)_4$, $Mo_2(chp)_4$ has an absorption 690 cm^{-1} below A_0 (Figure 6). In addition to the strong luminescence mentioned above, there is weak structured emission whose origin precisely overlaps the weak absorption feature 690 cm^{-1} below A_0 (Figure 10). The weak absorption and emission may be attributed to a triplet state. Either it is one spin–orbit component of the ^3E state (spin–orbit splitting, 280 cm^{-1}), and the strong emission is the other, or it is emission independent of the strong luminescent features. We tend to favor

(14) Craig, D. P.; Small, G. J. *J. Chem. Phys.* **1968**, *50*, 3827–3834. Small, G. J. *Ibid.* **1971**, *54*, 3300–3306. Sharf, B.; Honig, B. *Chem. Phys. Lett.* **1970**, *7*, 132–136.

(15) Miskowski, V. M.; Goldbeck, R. A.; Kliger, D. S.; Gray, H. B. *Inorg. Chem.* **1979**, *18*, 86–89.

(16) Trogler, W. C.; Solomon, E. I.; Gray, H. B. *Inorg. Chem.* **1977**, *16*, 3031–3033.

(17) Morgante, C. G.; Struve, W. S. *Chem. Phys. Lett.* **1979**, *63*, 344–346.

(18) Manning, M. C.; Holland, G. F.; Ellis, D. E.; Trogler, W. C. *J. Phys. Chem.*, in press.

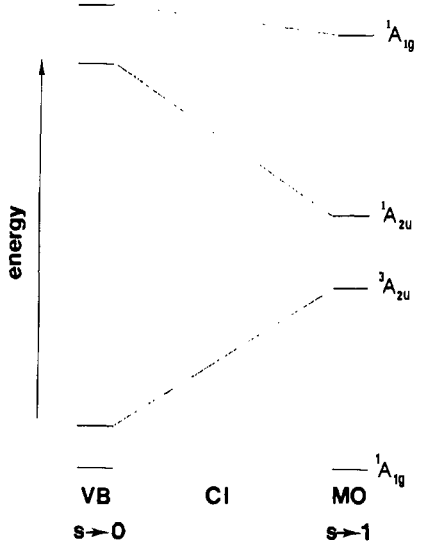

Figure 13. Correlation diagram for the δ,δ^* manifold. The configuration interaction regime (CI) is any situation between the MO and valence bond limits.

the latter rationale. A spin–orbit assignment is tenuous considering the additional weak luminescence is not present in $Mo_2(mhp)_4$. As a result, we rechecked the fluorescence spectra of $Mo_2(mhp)_4$. With use of excitation lines other than 5145 Å (used in spectra in Figure 7), a weak shoulder could be detected ~90 cm^{-1} below A_0 (Figure 12) in the emission spectrum. If the weak emission were a second spin-orbit component of the strong emission, then the magnitude of the spin–orbit splitting would have to be 3 times greater in $Mo_2(chp)_4$ than in $Mo_2(mhp)_4$, an unlikely occurrence. This weak shoulder may be the true origin of the anomalous D progression.

A weak absorption feature is seen in $W_2(mhp)_4$ as well, falling 600 cm^{-1} below A_0 (Figure 7). It cannot be seen in the film spectrum (Figure 8), either due to the band shifting or lack of resolution due to the long low-energy shoulder. Again, we would assign this band to a triplet absorption. A single, poorly resolved, emission is observed with characteristics similar to those of the $Mo_2(chp)_4$ band. Here we have further indication that the major emission is from the singlet $\delta\delta^*$ state. The gap between the 0–0 bands is ~600 cm^{-1}, which places it, perhaps coincidently, at the same energy as the $\delta \rightarrow \pi^*$ triplet state, obscuring the latter emission. Overall, we have data consistent with the $\delta\delta^*$ singlet state showing structured absorption and emission. The discrepancy in the Franck–Condon factors may be explained by an excited-state distortion, probably rotation from the eclipsed geometry toward a staggered geometry.

According to Table XII, the next two lowest singlet transitions should be $\delta \rightarrow \pi^*$ ($^1A_1 \rightarrow {}^1E$), $\delta \rightarrow \pi^*_{lig}$ ($^1A_1 \rightarrow {}^1E$), and $\pi \rightarrow \delta^*$ ($^1A_1 \rightarrow {}^1E$). In both molybdenum compounds, there is a band at ~405 nm with a distinct shoulder to higher energy (see Figure 13). These features can be seen in $W_2(mhp)_4$ as well, but now the gap between $\delta \rightarrow \delta^*$ and a second band system is quite small, and they appear as a double hump with a long high-energy tail. Each hump displays fine structure with the higher energy band having a marked reduction in progressional frequency relative to the first (280 vs. 320 cm^{-1}). We assign the second band to $\delta \rightarrow \pi^*$. Excitation into the π^* orbital should weaken the metal bond to a greater extent than $\delta \rightarrow \delta^*$, accounting for the decreased excited-state frequency. Assignment of the high-energy shoulder is more problematical as several alternatives (e.g., $\pi \rightarrow \delta^*$ or $\delta \rightarrow \pi^*_{ligand}$) can be imagined.

A Caveat on Resonance Raman. One disturbing observation was the lack of an appreciable resonance effect in the Raman spectra of the $M_2(mhp)_4$ and $Mo_2(chp)_4$ complexes. Previous success[12] with $Re_2X_8^{2-}$ (X = Cl, Br) and $Mo_2X_8^{4-}$ (X = Cl, Br) compounds suggested that resonance enhancement of the metal–metal stretch might serve as a useful diagnostic for the $\delta \rightarrow \delta^*$ absorption. Recently, we noted[18] the lack of such an enhancement in the spectra of $Mo_2(O_2CR)_4$ [R = H, CH_3, and CF_3] complexes; however, the weak intensity of the $\delta \rightarrow \delta^*$ absorption complicated the interpretation in this instance. In the present study the absorption spectral data shows that the $\delta \rightarrow \delta^*$ excited state exhibits a Franck–Condon distortion in the metal–metal stretch. The molar extinction coefficients are as high as 20 000 M^{-1} cm^{-1} for $W_2(mhp)_4$. Yet we fail to observe significant resonance Raman effects. It seems likely that the Raman line width factor (in the denominator for resonance Raman scattering) of these complexes is large. This indicates that the $\delta \rightarrow \delta^*$ excited state is strongly coupled to nearby excited states. In retrospect, this is not too surprising in view of the number of close lying excited states described above.

Overall Spectral Behavior. The absorption spectra of all four compounds in this study show remarkable similarity. A vibronically structured $\delta \rightarrow \delta^*$ absorption band appears as the lowest energy feature in all cases. Next, there is a more intense band with a distinct high energy shoulder. This band is somewhat obscured in the chromium case and has been assigned to $\delta \rightarrow \pi^*$

A distinguishable feature is the uniform bathochromic and hyperchromic trends of the lowest energy, structured $\delta \rightarrow \delta^*$ absorption in going from chromium through tungsten. Indeed, the tremendous range of intensities for the absorption helps to explain why the spectra of quadruply bonded complexes have been so difficult to interpret. In fact, for all quadruply bonded complexes, there appears to be a rough correlation between band position and energy, that is, the lower energy $\delta \rightarrow \delta^*$ excitations seem to be the most intense. In Table XIII, we have divided the compounds into three classes according to the molar extinction coefficient of this transition. Those with the weakest bands (class A) have oxygen donor ligands and excitation energies averaging ~21 000 cm^{-1} (475 nm). Class B compounds exhibit more varied band positions clustered around 19 000–20 000 cm^{-1} (510 nm). The more intense excitations occur in second- and third-row metals with good donor ligands (either σ or π donors, vide infra). Vertical transition energies average about 16 000 cm^{-1} (625 nm) for this class.

At first glance, this trend appears inverted. Upon going from class A to class C, one progresses to larger metals containing better donor ligands. These ligands will place more electron density on the metal centers, expand the valence shell, and increase δ overlap. However, for a bonding-to-antibonding type transition, one usually argues that increased overlap should blue shift the band. Simple, non-CI (configuration interaction) calculations predict a blue shift.[18,19] The apparent conflict between theory and experiment may lie in the small overlap in a δ bond. With use of the weak coupling model, the intrinsically small intensity of the fully allowed $\delta \rightarrow \delta^*$ transition could be rationalized.[1] Elegant calculations suggest that CI plays an important role in the correct description of the $\delta \rightarrow \delta^*$ excited state.[20,21] Molecular orbital theory occupies one of two extremes in describing excited states, working on the assumption that orbital overlap is very large (S → 1). At the other end of the spectrum, the valence bond approach presumes the opposite overlap limit (S → 0). Configuration interaction bridges these extreme descriptions. In Figure 13, we can see how the two models would describe the following four states in the usual D_{4h} symmetry: the ground state (δ^2, $^1A_{1g}$), the singlet and triplet components of the singly excited state ($\delta^1\delta^{*1}$, $^1A_{2u}$, $^3A_{2u}$), and the doubly excited state (δ^{*2}, $^1A_{1g}$). Valence bond theory has a very low-energy triplet (which is covalent in nature[22]) and very high-energy singlets (of ionic character, where both electrons reside on the same atomic site[22]). As overlap between the metals increases, the singlet drops in energy and gains more covalent character. Such behavior could explain the trend in Table XII. In class A type compounds, the overlap is very poor, and they are near the VB limit. As overlap increases, the energy drops (Figure

(19) Bursten, B. E.; Cotton, F. A. *Trans. Faraday Symp.* **1980**, *14*, 180–193.
(20) Hay, P. J. *J. Am. Chem. Soc.* **1978**, *100*, 2897–2898.
(21) Bernard, M. *J. Am. Chem. Soc.* **1978**, *100*, 2354–2362; *J. Chem. Phys.* **1979**, *71*, 2546–2550.
(22) Trogler, W. C. *J. Chem. Educ.* **1980**, *57*, 424–427.

Table XIII. Compilation of Band Positions and Molar Extinction Coefficients for the Lowest Energy Electronic Absorption Band ($\delta \rightarrow \delta^*$) in Quadruple Bond Metal Complexes

compound	energy, cm^{-1}	ϵ, M^{-1} cm^{-1}	M–M,[a] Å	ref
		Class A ($\epsilon \leq 220$ M^{-1} cm^{-1})		
$Cr_2(O_2CCH_3)_4 \cdot 2H_2O$	21 000	~80	2.836	13
$Mo_2(O_2CCF_3)_4$	23 000	120	2.090	*c*
$Mo_2(O_2CC_3F_7)_4$	23 000	100	...	*d*
$Mo_2(O_2CH)_4$	22 800	120	2.091	*e*
$Mo_2(O_2CCH_3)_4$	22 700	60	2.093	*d*
$Mo_2(O_2CCH_2NH_3)_4^{4+}$	22 600	95	2.115	*f*
	22 420	~100		*g*
$Mo_2(SO_4)_4^{4+}$	19 400	170	2.111	*h*
	19 400	150–250		*i*
$Re_2(O_2CEt)_4Cl_2$	20 120	157	*b*	*j*
$Re_2(O_2CEt)_4Br_2$	19 650	203	*b*	*j*
$Re_2(O_2C\text{-}n\text{-}Pr)_4Cl_2$	19 700	156	2.235	*j*
$Re_2(O_2C\text{-}n\text{-}Pr)_4Br_2$	19 700	153	2.234	*j*
$Re_2(O_2CC_6H_5)_4Cl_2$	18 750	220	2.235	*j*
		Class B (ϵ 250–1200 M^{-1} cm^{-1})		
$Mo_2^{4+}(H_2O)_x$	19 800	337	...	*g*
$Mo_2(H_2NCH_2CH_2NH_2)_4^{4+}$	21 100	480	*b*	*k*
$Mo_2(O_2CCH_3)_2Cl_4^{2-}$	20 200	490	2.086	27
$Cr_2(mhp)_4$	22 450	480	1.889	this work
$Mo_2(CH_2P(Me)_2CH_2)_4$	19 950	660	2.082	*l*, *m*
$Cr_2(CH_3)_8^{4-}$	22 000	≤700	1.980	*n*
$Re_2(O_2CCH_3)_4Cl_2$	15 750	755	2.209	*o*
$Re_2(O_2C\text{-}n\text{-}Pr)_4I_2$	19 530	790	...	*j*
$Re_2F_8^{2-}$	17 900	810	...	*p*
$Mo_2Cl_8^{4-}$	19 300	1050	2.134–2.150	*i*
$Mo_2Br_8^{4-}$	19 400	1170	2.135	*i*
		Class C (ϵ >1200 M^{-1} cm^{-1})		
$Re_2(CH_3)_8^{2-}$	18 600	≤1500	2.178	*n*
$Mo_2(CH_3)_8^{4-}$	19 500	≤1500	2.148	*n*
$Re_2(NCS)_8^{2-}$	10 000	1960	...	*q*
$Tc_2Cl_8^{2-}$	14 400	~2000	2.117	*r*
$Mo_2(mhp)_4$	19 800	2100	2.065	this work
$Re_2Cl_8^{2-}$	14 700	2340	2.222	*s*
		2480		*s*
		2770		*q*
		~2800		*j*
$Re_2I_8^{2-}$	12 800	~3000	...	*t*
$Mo_2(NCS)_8^{4-}$	14 500	~2600	2.162	*u*
$Mo_2Cl_4(PEtPh_2)_4$	16 720	3125	*b*	*v*
$Mo_2Cl_4(P\text{-}n\text{-}Bu_3)_4$	17 040	3150	*b*	*v*
$Mo_2Cl_4(PEt_3)_4$	17 040	3065	*b*	*v*
$Mo_2Cl_4(PMe_3)_4$	17 180	3400	2.130	*w*
$W_2Cl_4(PMe_3)_4$	15 210	4100	2.262	*w*
$W_2(mhp)_4$	17 500	~18 000	2.161	this work

[a] Bond lengths taken from ref 3. [b] Not known, but probably very similar to cogener listed below. [c] Cotton, F. A.; Norman, J. G. *J. Coord. Chem.* 1971, *1*, 161–172. [d] Dubicki, L.; Martin, R. L. *Aust. J. Chem.* 1969, *22*, 1571–1581. [e] Cotton, F. A.; Norman, J. G.; Stults, B. R.; Webb, T. R. *J. Coord. Chem.* 1976, *5*, 217–223. [f] Cotton, F. A.; Martin, D. S.; Webb, T. R.; Peters, T. J. *Inorg. Chem.* 1976, *15*, 1199–1201. [g] Cotton, F. A.; Webb, T. R. *Ibid.* 1976, *15*, 68–71. [h] Erwin, D. K.; Geoffroy, G. L.; Gray, H. B.; Hammond, G. S.; Solomon, E. I.; Trogler, W. C.; Zagars, A. A. *J. Am. Chem. Soc.* 1977, *99*, 3620–3621. [i] Trogler, W. C.; Erwin, D. K.; Geoffroy, G. L.; Gray, H. B. *Ibid.* 1978, *100*, 1160–1163. [j] Cotton, F. A.; Curtis, N. F.; Robinson, W. R. *Inorg. Chem.* 1966, *5*, 1798–1802. [k] Bowen, A. R.; Taube, H. *Ibid.* 1974, *13*, 2245–2249. [l] Cotton, F. A.; Fanwick, P. E. *J. Am. Chem. Soc.* 1979, *101*, 5252–5255. [m] Bohmer, W.-H.; Madeja, K.; Kurras, E.; Rosenthal, U. *Z. Chem.* 1978, *18*, 453–454. [n] Sattelberger, A. P.; Fackler, J. P. *J. Am. Chem. Soc.* 1977, *99*, 1258–1259. [o] Cotton, F. A.; Oldham, C.; Walton, R. A. *Inorg. Chem.* 1967, *6*, 214–223. [p] Preetz, W.; Peters, G. *Z. Naturforsch., B: Anorg. Chem., Org. Chem.* 1979, *34B*, 1767–1768. [q] Cotton, F. A.; Robinson, W. R.; Walton, R. A.; Whyman, R. *Inorg. Chem.* 1967, *6*, 929–935. [r] Preetz, W.; Peter, G. *Z. Naturforsch., B: Anorg. Chem., Org. Chem.* 1980, *35B*, 797–801. [s] Cotton, F. A.; Curtis, N. F.; Johnson, B. F. G.; Robinson, W. R. *Inorg. Chem.* 1965, *4*, 326–330. [t] Preetz, W.; Rudzik, L. *Angew. Chem., Int. Ed. Engl.* 1979, *18*, 150–151. [u] Bino, A.; Cotton, F. A.; Fanwick, P. E. *Inorg. Chem.* 1979, *18*, 3558–3562. [v] Trogler, W. C.; Gray, H. B. *Nouv. J. Chim.* 1977, *1*, 475–477. [w] Cotton, F. A.; Extine, M. W.; Felthouse, T. R.; Kolthammer, B. W. S.; Lay, D. G. *J. Am. Chem. Soc.* 1981, *103*, 4040–4045.

13) and absorption intensity is expected to increase as the overlap squared.[1]

What factors influence the increase in overlap? First, a descent in the periodic table will lead to larger metal d orbitals and better overlap. Second, the σ-electron-donating ability of the ligands can increase the effective charge on the metal, expand the d orbitals, and strengthen δ overlap. A nice illustration of the ligand effect may be found in Table XIII for $Re_2X_8^{2-}$ complexes (X = F, Cl, Br, I). While the δ levels showed an acute sensitivity to the nature of the ligand, the metal π orbitals apparently do so to a lesser extent. A possible explanation arises from ligand field theory. Quadruply bonded compounds can be approximated as face-to-face dimers of square-planar complexes. As the ligands approach the metal along the x and y axes, they interact directly with the $d_{x^2-y^2}$ and d_{z^2} orbitals to form metal-to-ligand σ bonds and perturb these particular d orbitals to the greatest extent. The orbital affected to the next greatest extent is the coplanar d_{xy} function used to form the metal–metal δ bond.[26]

Simple σ donation is not the only ligand effect to be considered. If this were the case, then the alkyl derivatives would be expected to possess the most intense $\delta \rightarrow \delta^*$ absorption. Compounds which have anamolously strong $\delta \rightarrow \delta^*$ bands include the halide derivatives, and particularly, the mhp complexes. Both the halide ligands and mhp can act as π donors. The pyridine ring of mhp has a filled π shell which can directly repel the filled δ orbital. This may push more δ electron density into the metal–metal

bonding region. The p electrons on the halide ligands could function in a similar manner, although apparently to a lesser degree.

The aforementioned overlap effects, while greatly influencing the electronic spectra, particularly the portion associated with the δ orbitals, may not play an important role in determining bond lengths or bond strengths (as measured by force constants or thermodynamic methods). These latter properties are probably set by the much stronger σ and π interactions, which maximize at longer metal-metal distances than δ interactions. A number of examples are apparent in the literature,[23-25] where the strength, or even the existence, of the δ orbital has little or no effect on metal-metal bond strength.

In the following series:[27]

	$Mo_2(O_2CCH_3)_4$	$Mo_2(O_2CCH_3)_2Cl_4^{2-}$	$Mo_2Cl_8^{4-}$
M-M, Å	2.093	2.086	2.14
$\delta \rightarrow \delta^*$, cm^{-1}	22 700	20 200	19 300
ϵ, M^{-1} cm^{-1}	105	490	1050

there is no correlation of the $\delta \rightarrow \delta^*$ absorption energy with the bond length. Some previous work[28] has emphasized the linear relation between the $\delta \rightarrow \delta^*$ absorption energy and the metal-metal bond length within a restricted series of compounds. This is quite a reasonable hypothesis, and we note a similar excellent linear correlation for the $M_2(mhp)_4$ systems we have studied. However, the IP of the δ electrons correlates just as well as the metal-metal bond length for the $M_2(mhp)_4$ systems. Because of chemical periodicity, it is clear that many physical properties will tend to parallel one another. In this paper we have presented what we believe are the fundamental parameters which influence the position and intensity of the $\delta \rightarrow \delta^*$ transition.

Acknowledgment. We thank the National Science Foundation for financial support.

Registry No. $Cr_2(mhp)_4$, 67634-82-6; $Mo_2(mhp)_4$, 67634-80-4; $W_2(mhp)_4$, 67634-84-8; $Mo_2(chp)_4$, 73274-69-8.

Supplementary Material Available: Tables of spectral data and absorption spectra of $Mo_2(chp)_4$ and Hchp in tetrahydrofuran, $Mo_2(mhp)_4$ in an argon matrix at 10 K, $Mo_2(mhp)_4$ in a nitrogen matrix at 10 K, $Mo_2(mhp)_4$ in a xenon matrix at 10 K, and $W_2(mhp)_4$ in an argon matrix at 10 K (8 pages). Ordering information is given on any current masthead page.

(23) Cotton, F. A.; Davison, A.; Day, V. W.; Fredrich, M. F.; Orvig, C.; Swanson, R. *Inorg. Chem.* **1982**, *21*, 1211-1214.
(24) Cotton, F. A.; Frenz, B. A.; Ebner, J. R.; Walton, R. A. *Inorg. Chem.* **1976**, *15*, 1630-1633.
(25) Lichtenberger, D. L., reported at Inorganic Chemistry Biennial Symposium, Indiana University, May 16-19, 1982.
(26) Zuckerman, J. J. *J. Chem. Educ.* **1965**, *42*, 315-317. Krishnamurthy, R.; Schaap, W. B. *Ibid.* **1969**, *46*, 799-810.
(27) Clegg, W.; Garner, C. D.; Parkes, S.; Walton, I. B. *Inorg. Chem.* **1979**, *18*, 2250-2255.
(28) Sattelberger, A. P.; Fackler, J. P. *J. Am. Chem. Soc.* **1977**, *99*, 1258-1259.

Isolation and Crystal Structures of the Halide-Free and Halide-Rich Phenyllithium Etherate Complexes $[(PhLi\cdot Et_2O)_4]$ and $[(PhLi\cdot Et_2O)_3\cdot LiBr]$†

Håkon Hope and Philip P. Power*

Contribution from the Department of Chemistry, University of California at Davis, Davis, California 95616. *Received December 27, 1982*

Abstract: The compounds $[(PhLi\cdot Et_2O)_4]$ and $[(PhLi\cdot Et_2O)_3\cdot LiBr]$ have been isolated, and characterized by single-crystal X-ray studies. The $[(PhLi\cdot Et_2O)_4]$ crystals possess monoclinic symmetry of space group $I2/a$, $Z = 4$, with $a = 20.043$ (18) Å, $b = 9.707$ (8) Å, $c = 20.498$ (16) Å, and $\beta = 96.66$ (7)°. The structure consists of two interlocking tetrahedra of four lithium and four phenyl carbon atoms in a distorted cubane framework. Each lithium is further coordinated by oxygen from an ether molecule. The coordination at lithium is approximately tetrahedral. The $[(PhLi\cdot Et_2O)_3\cdot LiBr]$ crystals are also monoclinic of space group $P2_1/c$, $Z = 4$, with $a = 18.632$ (4) Å, $b = 7.709$ (2) Å, $c = 22.253$ (8) Å, and $\beta = 94.63$ (3)°. In the case of $[(PhLi\cdot Et_2O)_3\cdot LiBr]$ the framework is further distorted by the presence of Br^- instead of a carbon from a phenyl group. The lithium diagonally opposite Br^- in the cube is uncoordinated by ether. This is the first structure report for an organolithium halide complex.

The chemical constitution of the lithium alkyls and aryls and the nature of their structure in solution or in the solid phase have been outstanding problems in organometallic chemistry.[1] Much of the published work has concentrated upon the alkyl derivatives, and a number of crystal structures have appeared.[2] Studies of aryllithium compounds in solution involving both ultraviolet and NMR spectroscopy have been reported.[3,4] In addition, vapor pressure and ebulliosocopic work have established that the degree of association of such compounds in diethyl ether or tetrahydrofuran is two, whereas for the alkyl derivatives it is either four or six.[5,6] However, the structure of phenyllithium has not been established with certainty either in solution or in the crystalline state.

† No reprints available.

(1) Wakefield, B. J. "The Chemistry of Organolithium Compounds"; Pergamon Press: New York, 1974. Coates, G. E.; Wade, K. "Organometallic Compounds"; Methuen: London, 1967. Wardell, J. L. "Comprehensive Organometallic Chemistry"; Pergamon Press: New York, 1982; Vol. 1, Chapter 2, pp 43-121. Brown, T. L. *Pure Appl. Chem.* **1970**, *23*, 447-462. Oliver, J. P. *Adv. Organomet. Chem.* **1977**, *15*, 235-271.
(2) Weiss, E.; Hencken, G. *J. Organomet. Chem.* **1970** *21*, 265-8. Dietrich, H. *Acta Crystallogr.* **1963**, *16*, 681-9.
(3) Fraenkel, G.; Adams, D. G.; Dean, R. R. *J. Phys. Chem.* **1968**, *72*, 944-53. Fraenkel, G.; Dayagi, F. S.; Kobayashi, S. *Ibid.* **1968**, *72*, 953-61.
(4) Ladd, J. A. *Spectrochim. Acta* **1966**, *22*, 1157-63. Parker, J.; Ladd, J. A. *J. Organomet.* Chem. **1969**, *19*, 1-7.

0002-7863/83/1505-5320$01.50/0